COLD SPRING HARBOR
Molecular Case Studies

RESEARCH ARTICLE

Disease-associated mosaic variation in clinical exome sequencing: a two-year pediatric tertiary care experience

Cecelia R. Miller,[1,2] Kristy Lee,[1,2] Ruthann B. Pfau,[1,2,3] Shalini C. Reshmi,[1,2,3] Donald J. Corsmeier,[1] Sayaka Hashimoto,[1] Ashita Dave-Wala,[1] Vijayakumar Jayaraman,[1] Daniel Koboldt,[1,3] Theodora Matthews,[1] Danielle Mouhlas,[1] Maggie Stein,[1] Aimee McKinney,[1] Tom Grossman,[1] Benjamin J. Kelly,[1] Peter White,[1,3] Vincent Magrini,[1,3] Richard K. Wilson,[1,3] Elaine R. Mardis,[1,3] and Catherine E. Cottrell[1,2,3]

[1]The Steve and Cindy Rasmussen Institute for Genomic Medicine, Nationwide Children's Hospital, Columbus, Ohio 43205, USA; [2]Department of Pathology, [3]Department of Pediatrics, The Ohio State University, Columbus, Ohio 43210, USA

Abstract Exome sequencing (ES) has become an important tool in pediatric genomic medicine, improving identification of disease-associated variation due to assay breadth. Depth is also afforded by ES, enabling detection of lower-frequency mosaic variation compared to Sanger sequencing in the studied tissue, thus enhancing diagnostic yield. Within a pediatric tertiary-care hospital, we report two years of clinical ES data from probands evaluated for genetic disease to assess diagnostic yield, characteristics of causal variants, and prevalence of mosaicism among disease-causing variants. Exome-derived, phenotype-driven variant data from 357 probands was analyzed concurrent with parental ES data, when available. Blood was the source of nucleic acid. Sequence read alignments were manually reviewed for all assessed variants. Sanger sequencing was used for suspected de novo or mosaic variation. Clinical provider notes were reviewed to determine concordance between laboratory-reported data and the ordering provider's interpretation of variant-associated disease causality. Laboratory-derived diagnostic yield and provider-substantiated diagnoses had 91.4% concordance. The cohort returned 117 provider-substantiated diagnoses among 115 probands for a diagnostic yield of 32.2%. De novo variants represented 64.9% of disease-associated variation within trio analyses. Among the 115 probands, five harbored disease-associated somatic mosaic variation. Two additional probands were observed to inherit a disease-associated variant from an unaffected mosaic parent. Among inheritance patterns, de novo variation was the most frequent disease etiology. Somatic mosaicism is increasingly recognized as a significant contributor to genetic disease, particularly with increased sequence depth attainable from ES. This report highlights the potential and importance of detecting mosaicism in ES.

[Supplemental material is available for this article.]

Corresponding author: Catherine.cottrell@nationwidechildrens.org

Ontology terms: autism; delayed gross motor development; failure to thrive in infancy; microcephaly; profound global developmental delay; severe muscular hypotonia; short stature

Published by Cold Spring Harbor Laboratory Press

doi:10.1101/mcs.a005231

INTRODUCTION

Massively parallel sequencing (MPS) of the exome has demonstrated significant diagnostic and clinical utility in patients with suspected genetic disorders (Lee et al. 2014; Farwell et al. 2015; Meng et al. 2017; Clark et al. 2018; Hu et al. 2018). Molecular diagnostic rates from clinical testing by hospital and reference laboratories performing exome sequencing (ES) range from 24%

to 58%, likely influenced by laboratory-specific methodologies and by the characteristics of the patient population being evaluated (Clark et al. 2018). Given the utility of ES, it has been proposed that the assay should be considered as a first-tier molecular test (Stark et al. 2016; Hu et al. 2018). An additional advantage to this type of testing is the ability to reevaluate existing sequence data as advances in bioinformatic processing and variant detection occur over time. Furthermore, this approach allows for a consideration of the evolution of patient phenotype, in addition to the inclusion of updated/emerging data for disease–gene associations, thus further enhancing diagnostic potential (Ewans et al. 2018; Nambot et al. 2018).

The increased utilization of MPS, including ES, has expanded our understanding of the contribution of somatic mosaicism in genetic disorders by enhancing our ability to identify disease-associated variants at low variant allele frequency/fraction (VAF). Genetic variation acquired during embryogenesis and resulting in the establishment of two or more genetically distinct cell populations represents postzygotic mosaicism. Disease-causing variants can be confined to the germline (gonadal mosaicism), resulting in disease when passed on to subsequent offspring. Alternatively, a genetic variant can occur in the soma of a developing embryo (somatic mosaicism), with variable levels of the variant throughout the body dependent on cell lineage. In addition, a mosaic variant affecting both the soma and germline is referred to as gonosomal mosaicism (Biesecker and Spinner 2018). The phenotypic spectrum of postzygotic somatic mosaicism can vary and is dependent upon timing of the manifestation of the variant during development, along with the proportion of cells harboring the variant and distribution across tissue types. Pathogenic variants at very low VAF in affected tissue can be sufficient to cause disease. For example, in diseases such as Sturge–Weber or vascular anomalies with overgrowth (e.g., Proteus syndrome or *PIK3CA*-related overgrowth spectrum [PROS]), the VAF of pathogenic variants in affected tissue has been reported as low as 1% (Lindhurst et al. 2011; Shirley et al. 2013; Hucthagowder et al. 2016).

Among unselected clinical exome cohort studies of pediatric, and combined pediatric and adult populations, disease-associated mosaic variants were noted at a frequency of ~1%–1.5% (Yang et al. 2013; Retterer et al. 2016; Cao et al. 2019). The frequency of mosaicism increases when examining for specific phenotypes. For example, in epilepsy-related neurodevelopmental disorders, 3% of the pathogenic variants identified by either an MPS epilepsy panel or ES were mosaic (Stosser et al. 2018). In certain disorders (e.g., McCune–Albright and PROS), mosaic variants are the primary mechanism of disease (Aldred and Trembath 2000; Keppler-Noreuil et al. 2015; Hucthagowder et al. 2016).

We evaluated two years of clinical ES data from our laboratory within a pediatric tertiary care center to determine the characteristics of disease-associated variants within our cohort, as well as to compare the diagnostic yield reported by the laboratory versus the ordering clinical provider's interpretation of laboratory reported variant causality. We sought to evaluate the concordance of the molecular ES diagnostic rate generated by the laboratory with clinical provider-confirmed diagnoses recorded in the electronic medical record (EMR) to test if the laboratory workflow, including selection of genes relevant to the proband phenotype and subsequent variant assessment, resulted in meaningful results being reported back to the ordering provider. We further summarized the characteristics of these provider-confirmed causal variants and evaluated the contribution of mosaic variants to genetic disease within the context of these diagnoses.

RESULTS

Patient Cohort

In a consecutive 24-month period, proband ($n = 357$) and parental (when available, $n = 601$) peripheral blood samples were submitted for ES to The Steve and Cindy Rasmussen Institute

for Genomic Medicine at Nationwide Children's Hospital, Columbus, Ohio. Two submitted parental samples were excluded because of nonpaternity. Cases represented 267 (74.8%) trio analyses of the proband plus both parental samples, 65 (18.2%) duo analyses of the proband and one parental sample, and 25 (7%) proband-only analyses. All cases were reviewed or referred by a clinical geneticist at the time of test order. The cohort consisted primarily of pediatric probands or young adults with symptoms that initially presented in childhood (average age = 7.2 yr, range 0–56 yr). A phenotype-informed approach was applied for tertiary analysis. The top 20 Human Phenotype Ontology (HPO) terms representing the most common clinician-provided phenotypic characteristics among probands in this population are shown in Table 1. Consistent with other ES cohorts, global developmental delay (73.4% of our cohort), abnormal facial shape (51.3%), and muscular hypotonia (51.0%) were the most frequently described features (Lee et al. 2014; Yang et al. 2014; Farwell et al. 2015).

Genomic Analyses

The clinical laboratory reported variants as likely causal for the proband's phenotype for 128 genetic disorders among 123 probands (34.5%; 95% CI, 29.5%–39.6%). Ordering provider documentation in the EMR corroborated 115 instances of the variant(s) being attributed to the etiology of the proband phenotype for a provider-substantiated diagnostic yield of 32.2% (95% CI, 27.4%–37.3%). Two probands were found to have two separate genetic disorders, for a total of 117 clinically confirmed genetic diagnoses. Clinical laboratory diagnoses and provider-substantiated diagnoses had an overall concordance of 91.4% [95% CI, 85.1%–95.6%]. Of the 11 laboratory-reported genetic disorders not substantiated by clinician data in the EMR, five were due to insufficient overlap of features, four remained in

Table 1. Frequency of the top 20 Human Phenotype Ontology (HPO) terms used to describe features of 357 probands referred for exome sequencing

HPO ID	HPO term	Number of probands (%)
HP:0001263	Global developmental delay	262 (73.4)
HP:0001999	Abnormal facial shape	183 (51.3)
HP:0001252	Muscular hypotonia	182 (51.0)
HP:0000750	Delayed speech and language development	157 (44.0)
HP:0001270	Motor delay	136 (38.1)
HP:0002194	Delayed gross motor development	127 (35.6)
HP:0001250	Seizures	119 (33.3)
HP:0100543	Cognitive impairment	98 (27.5)
HP:0001508	Failure to thrive	91 (25.5)
HP:0004322	Short stature	90 (25.2)
HP:0007010	Poor fine motor coordination	77 (21.6)
HP:0000252	Microcephaly	74 (20.7)
HP:0002020	Gastroesophageal reflux	69 (19.3)
HP:0000729	Autistic behavior	69 (19.3)
HP:0000717	Autism	59 (16.5)
HP:0001290	Generalized hypotonia	57 (16.0)
HP:0001622	Premature birth	56 (15.7)
HP:0002019	Constipation	56 (15.7)
HP:0001510	Growth delay	52 (14.6)
HP:0002376	Developmental regression	50 (14.0)

the differential for further clinical evaluation as the proband features develop, and two had discordant inheritance patterns among affected/unaffected family members. A diagnosis was determined for 10/25 (40.0%) of the proband-only analyses, 10/65 (15.4%) duo analyses, and 95/267 (35.6%) trio analyses. The patterns of inheritance for the 117 diagnoses included 75 (64.1%) autosomal dominant, 25 (21.4%) autosomal recessive, and 17 (14.5%) X-linked (Fig. 1).

Out of the 916 individuals consented for medically actionable findings, 29 individuals (3.2%) had variants meeting American College of Medical Genetics and Genomics (ACMG)/Association for Molecular Pathology (AMP) criteria supportive of a Pathogenic/Likely Pathogenic classification. Eight families demonstrated a proband–parent shared finding, whereas four probands and nine parents harbored events individually. Diseases represented by these findings were Loey–Dietz syndrome (4%), malignant hyperthermia susceptibility (10%), hypertrophic cardiomyopathy (10%), familial hypercholesterolemia (14%), arrhythmogenic right ventricular cardiomyopathy (14%), long QT syndromes (24%), and hereditary breast and ovarian cancer (24%).

Among 95 diagnostic ES trio studies, we identified 97 genetic disorders, of which the inheritance patterns were autosomal dominant ($n = 62$; 63.9%), autosomal recessive ($n = 21$; 21.7%), and X-linked ($n = 14$; 14.4%). Among the autosomal dominantly inherited diseases, 54 variants (87.1%) were confirmed as de novo, whereas nine (64.3%) of the X-linked inherited disorders were attributable to de novo variation. Overall, de novo variation accounted for 64.9% [63/97, 95% CI, 54.6%–74.4%] of the inheritance pattern of genetic disorders detected in trio ES.

Of the 117 disorders, genetic disease associations were diverse among this cohort with 65% of the identified disease-associated genetic loci unique to a single proband. Recurrently involved genetic loci included *CREBBP*, in which causal variants associated with Rubenstein–Taybi syndrome were identified in three probands. Additionally, four probands each had causal variants in *ANKRD11* and *IQSEC2*, associated with KBG syndrome and X-linked intellectual disability, respectively. Causal variants of provider-substantiated diagnoses are provided in Table 2 and Table 3, with the most common HPO terms describing this cohort detailed in Table 1.

The proportion of the causal variant allele was documented for proband and parental samples from all cases with a provider-substantiated diagnosis by evaluation of VAF.

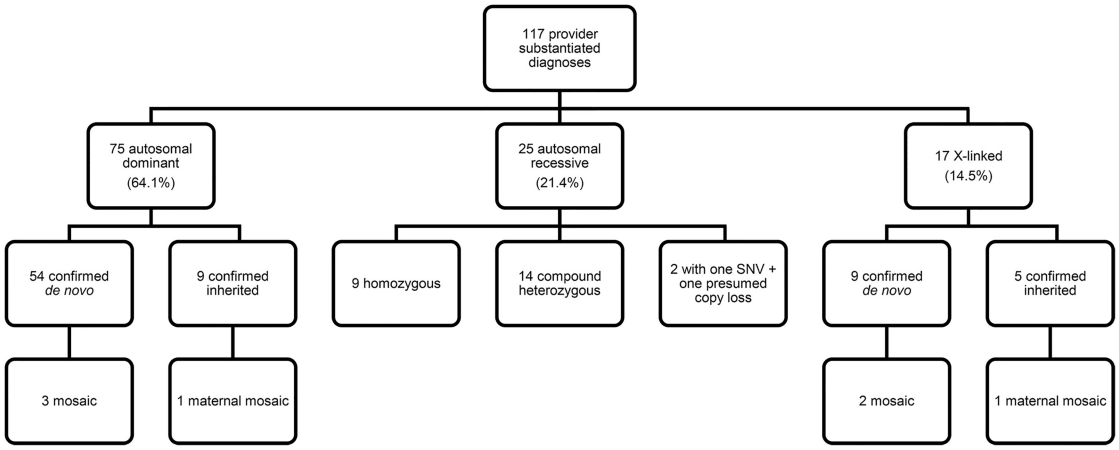

Figure 1. Distribution of variant types for 117 provider-substantiated diagnoses identified by exome sequencing in a pediatric cohort. (SNV) Single-nucleotide variant.

Table 2. Summary of cases with a pathogenic or likely pathogenic mosaic variant in a proband or parental sample

Case	Proband gender/ age	Clinical phenotype	Gene	Zygosity/ VAF	Chromosome (hg19)	HGVS DNA and protein reference	Variant type/ predicted effect	Parent of origin/ VAF	Relevant disease association	Supporting references
1	Male/6 mo	Failure to thrive, profound hypotonia, global developmental delay, microcephalic, bilateral esotropia, short palpebral fissures, protuberant tongue, sparse scalp hair, hypsarrhythmia by long-term electroencephalographic monitoring, delayed myelination on MRI	*ARX*	Mosaic (12%)	Chr X:25025232 C > T	NM_139058.2 c.1444G > A p.(Gly482Ser)	Substitution/ missense	De novo	(XL) Early infantile epileptic encephalopathy 1	Shoubridge et al. 2012; Shoubridge et al. 2010; Gronskov et al. 2014; Poirier et al. 2005
2	Male/11 yr	Generalized epilepsy, global developmental delay, intellectual disability, autism, attention deficit hyperactivity disorder, able to walk independently with orthotics and verbally communicate	*CDKL5*	Mosaic (17%)	Chr X:18602452 G > A	NM_003159.2 c.533G > A p.(Arg178Gln)	Substitution/ missense	De novo	(XL) Early infantile epileptic encephalopathy 2	Bahi-Buisson et al. 2012; Kilstrup-Nielsen et al. 2012; Mei et al. 2014; Masliah-Plachon et al. 2010; Stosser et al. 2018; Kothur et al. 2018; Olson et al. 2019
3	Male/1 yr	Global developmental delay, seizures, chorea, hypotonia, short stature, poor feeding, ptosis, frontal bossing, micrognathia	*TRIP12*	Mosaic (12%)	Chr 2:230679862 G > A	NM_004238.2 c.1540C > T p.(Arg514Ter)	Substitution/ nonsense	De novo	(AD) Clark–Baraitser syndrome	Bramswig et al. 2017a; Zhang et al. 2017; Louie et al. 2020
4	Male/7 yr	Localization-related partial epilepsy with complex partial seizures, nonambulatory, global developmental delay, postnatal growth retardation, intellectual disability, autism, hyperopia, chronic constipation, dysphagia	*IQSEC2*	Hemi (98%)	Chr X:53264051 G > A	NM_001111125.2 c.3817C > T p.(Gln1273Ter)	Substitution/ nonsense	Mosaic mother (11%)	(XL) Mental retardation 1	Barrie et al. 2019[a]; Ewans et al. 2017; Radley et al. 2019; Mignot et al. 2019

(*Continued on next page.*)

Table 2. (*Continued*)

Case	Proband gender/ age	Clinical phenotype	Gene	Zygosity/ VAF	Chromosome (hg19)	HGVS DNA and protein reference	Variant type/ predicted effect	Parent of origin/ VAF	Relevant disease association	Supporting references
5	Female/8 yr	Global developmental delay, fine motor delay, hirsutism, agenesis of the corpus callosum, hypotonia, tethered spinal cord, exotropia, clubfoot, tall forehead, downslanting palpebral fissures, macrostomia	*ARID1A*	Mosaic (19%)	Chr 1:27092947 G > A	NM_139135.2 c.2879-1G > A p.?	Substitution/ splicing	De novo	(AD) Coffin–Siris syndrome 2	Tsurusaki et al. 2012; Santen et al. 2013; Wieczorek et al. 2013
6	Male/7 yr	Periventricular white matter changes on MRI, mild intellectual disability, global developmental delay, hypotonia, GERD, myopathic facies, thickened low-set ears, flared nasal alae, upturned nasal tip	*ARID2*	Het (46%)	Chr 12: 46245833_ 46245834delAG	NM_152641.3 c.3927_3928delAG p.(Gly1310Glufs Ter5)	Deletion/ frameshift	Mosaic mother (4%)	(AD) Coffin–Siris syndrome 6	Tsurusaki et al. 2012; Bramswig et al. 2017b; Bogershausen and Wollnik 2018
7	Female/ 2 yr	Macrocephaly, hirsutism, global developmental delay, bilateral perisylvian polymicrogyria with mildly enlarged ventricles on MRI	*PIK3R2*	Mosaic (18%)	Chr 19:18273784 G > A	NM_005027.3 c.1117G > A p.(Gly373Arg)	Substitution/ missense	De novo	(AD) Megalencephaly-polymicrogyria-polydactyly-hydrocephalus syndrome 1	Mirzaa et al. 2015; Riviere et al. 2012; Madsen et al. 2018

(VAF) Variant allele frequency/fraction, (hemi) hemizygous, (het) heterozygous, (N/A) not applicable, (XL) X-linked, (AD) autosomal dominant, (MRI) magnetic resonance imaging, (GERD) gastroesophageal reflux disease.
[a]Case previously reported.

Table 3. Summary of causal variants in a pediatric exome cohort

Case	Study type	Gene	Chromosome (hg19)	HGVS DNA and protein reference	Zygosity	Parent of origin	Relevant disease association	Variant assessment	ACMG/AMP criteria met
Autosomal recessive (homozygous)									
8[a]	Trio	*AMPD2*	Chr 1:110172910 C > T	NM_001257360.1 c.2201C > T p.(Pro734Leu)	Hom	Mat/pat	(AR) Pontocerebellar hypoplasia, type 9 (OMIM: 615809); (AR) ? Spastic paraplegia 63 (OMIM: 615686)	VUS	PM2, PP3
		COL11A1	Chr 1:103488375 C > A	NM_080629.2 c.1204G > T p.(Glu402Ter)	Hom	Mat/pat	(AD) Stickler syndrome, type II (OMIM: 604841) (AR) fibrochondrogenesis 1 (OMIM: 228520); (AD) Marshall syndrome (OMIM: 154780)	Likely pathogenic	PVS1, PM2
9	Trio	*AP4S1*	Chr 14:31542174 C > T	NM_001254727.1 c.289C > T p.(Arg97Ter)	Hom	Mat/pat	(AR) Spastic paraplegia 52, autosomal recessive (OMIM: 614067)	Pathogenic	PVS1, PM2, PM3, PP1
10	Trio	*HYLS1*	Chr 11:125769895 A > G	NM_145014.2 c.632A > G p.(Asp211Gly)	Hom	Mat/pat	(AR) Hydrolethalus syndrome (OMIM: 236680)	Pathogenic	PS3, PM1, PS4_Moderate, PP1, PP3, PP5
11	Trio	*IDUA*	Chr 4:996535 G > A	NM_000203.4 c.1205G > A p.(Trp402Ter)	Hom	Mat/pat	(AR) Mucopolysaccharidosis Ih (OMIM: 607014); (AR) mucopolysaccharidosis Ih/s (OMIM: 607015); (AR) Mucopolysaccharidosis Is (OMIM: 607016)	Pathogenic	PVS1, PS3, PS4_Moderate, PP5
12[a]	trio	*KERA*	Chr 12:91449224 G > A	NM_007035.3 c.835C > T p.(Arg279Ter)	Hom	Mat/pat	(AR) Cornea plana 2, autosomal recessive (OMIM: 217300)	Pathogenic	PVS1, PM2, PS4_Moderate, PP1
		POLR3B	Chr 12:106850924 C > T	NM_018082.5 c.2302C > T p.(Arg768Cys)	Hom	Mat/pat	(AR) Leukodystrophy, hypomyelinating, 8, with or without oligodontia and/or hypogonadotropic hypogonadism (OMIM: 614381)	Likely Pathogenic	PM2, PM5, PP2, PP3
13	Trio	*PARN*	Chr 16:14704607 G > A	NM_002582.3 c.448C > T p.(Arg150Cys)	Hom	Mat/pat	(AR) Dyskeratosis congenita, autosomal recessive 6 (OMIM: 616353)	Likely Pathogenic	PM1, PM2, PS3_Moderate, PP3
14	Singleton	*PYCR1*	Chr 17:79892603 C > T	NM_001282281.1 c.640G > A p.(Ala214Thr)	Hom	Unknown	(AR) Cutis laxa, autosomal recessive, type IIB (OMIM: 612940) (AR) Cutis laxa, autosomal recessive, type IIIB (OMIM: 614438)	VUS	PM1, PM2, PP3
Autosomal recessive (compound heterozygous)									
15	Trio	*AP4M1*	Chr 7:99704117 C > T	NM_004722.3 c.1117C > T p.(Gln373Ter)	Het	Pat	(AR) Spastic paraplegia 50, autosomal recessive (OMIM: 612936)	Pathogenic	PVS1, PM2, PM3
		AP4M1	Chr 7:99704464 C > T	NM_004722.3 c.1321C > T p.(Arg441Ter)	Het	Mat	(AR) Spastic paraplegia 50, autosomal recessive (OMIM: 612936)	Likely pathogenic	PM2, PM3, PP3, PP5
16	Singleton	*HBB*	Chr 11:5248232 T > A	NM_000518.4 c.20A > T p.(Glu7Val)	Het	Unknown	(AR) Sickle cell anemia (OMIM: 603903)	Pathogenic	PS3, PM3, PM5, PS4_Moderate, PP5
		HBB	Chr 11:5246908 C > T	NM_000518.4 c.364G > A p.(Glu122Lys)	Het	Unknown	(AR) Sickle cell anemia (OMIM: 603903)	Likely pathogenic	PS4, PM2, PM3, PP5

(*Continued on next page.*)

Table 3. (*Continued*)

Case	Study type	Gene	Chromosome (hg19)	HGVS DNA and protein reference	Zygosity	Parent of origin	Relevant disease association	Variant assessment	ACMG/AMP criteria met
17	Trio	*MED25*	Chr 19:50331716 G > A	NM_030973.3 c.316G > A p.(Gly106Arg)	Het	Pat	(AR) ?Charcot–Marie–Tooth disease, type 2B2 (OMIM: 605589); (AR) Base–Vanagait–Smirin–Yosef syndrome (OMIM: 616449)	Likely pathogenic	PM2, PM3, PP2, PM5
		MED25	Chr 19:50338388_50338397 delACCACAAGCA	NM_030973.3 c.1628_1637delACCACAAGCA p.(Asn543ArgfsTer51)	Het	Mat	(AR) ?Charcot–Marie–Tooth disease, type 2B2 (OMIM: 605589); (AR) Basel–Vanagait–Smirin–Yosef syndrome (OMIM: 616449)	Likely pathogenic	PVS1, PM2
18	Duo	*OPA1*	Chr 3:193374977 delA	NM_130837.2 c.2287delA p.(Ser763ValfsTer15)	Het	Unknown	(AR) Behr syndrome (OMIM: 210000); (AR) optic atrophy 1 (OMIM: 165500); (AR) optic atrophy plus syndrome (OMIM: 125250)	Pathogenic	PVS1, PM2
		OPA1	Chr 3:193361167 A > G	NM_130837.2 c.1311A > G p.(Ile437Met)	Het	Mat	(AR) Behr syndrome (OMIM: 210000) ;(AR) optic atrophy 1 (OMIM: 165500); (AR) optic atrophy plus syndrome (OMIM: 125250)	VUS	PM1, PM3, PP1, PP3; BS3
19	Trio	*RYR1*	Chr 19:38951159 delG	NM_000540.2 c.2505delG p.(Pro836LeufsTer48)	Het	Pat	(AR) Minicore myopathy with external ophthalmoplegia (OMIM: 255320) (AD, AR) Central core disease (OMIM: 117000)	Pathogenic	PVS1, PM2, PP5
20	Trio	*RYR1*	Chr 19:38987047 A > G	NM_000540.2 c.6664-2A > G p.?	Het	Pat	(AR) Minicore myopathy with external ophthalmoplegia (OMIM: 255320); (AD, AR) central core disease (OMIM: 117000)	Pathogenic	PVS1, PM2, PP3
		RYR1	Chr 19.39075637 G > A	NM_000540.2 c.14701G > A p.(Glu4901Lys)	Het	Mat	(AR) Minicore myopathy with external ophthalmoplegia (OMIM: 255320); (AD, AR) central core disease (OMIM: 117000)	Likely pathogenic	PM1, PM3, PP2, PP3
21	Trio	*SAMHD1*	Chr 20:35563513 C > T	NM_015474.3 c.428G > A p.(Arg143His)	Het	Mat	(AR) Aicardi–Goutieres syndrome 5 (OMIM: 612952)	Pathogenic	PS3, PM2, PM5, PP3, PP5
		SAMHD1	Chr 20:35533834 A > G	NM_015474.3 c.1343T > C p.(Ile448Thr)	Het	Pat	(AR) Aicardi-Goutieres syndrome 5 (OMIM: 612952)	Likely pathogenic	PM2, PM3, PP3, PP4
22	Duo	*SLC17A5*	Chr 6:74351533 T > C	NM_012434.4 c.406A > G p.(Lys136Glu)	Het	Unknown	(AR) Salla disease (OMIM: 604369); (AR) sialic acid storage disorder, infantile (OMIM: 269920)	Pathogenic	PS3, PM2, PS4_Moderate, PP3, PP5
		SLC17A5	Chr 6:74345115 A > T	NM_012434.4 c.809T > A p.(Leu270Ter)	Het	Mat	(AR) Salla disease (OMIM: 604369); (AR) sialic acid storage disorder, infantile (OMIM: 269920)	Pathogenic	PVS1, PM2, PM3
23	Trio	*SLC22A5*	Chr 5:131706028 G > T	NM_003060.3 c.364G > T p.(Asp122Tyr)	Het	Mat	(AR) Carnitine deficiency, systemic primary (OMIM: 212140)	Likely pathogenic	PS3, PM2, PM3, PP3
		SLC22A5	Chr 5:131721062 C > T	NM_003060.3 c.695C > T p.(Thr232Met)	Het	Pat	(AR) Carnitine deficiency, systemic primary (OMIM: 212140)	Pathogenic	PS3, PM_PS4, PM2, PP3, PP5
24	Trio	*SLC6A3*	Chr 5:1422127 C > T	NM_001044.4 c.656G > A p.(Arg219His)	Het	Mat	(AR) Parkinsonism-dystonia, infantile, 1 (OMIM: 613135)	VUS	PM2, PP2, PP3
		SLC6A3	Chr 5:1416253 C > G	NM_001044.4 c.991G > C p.(Ala331Pro)	Het	Pat	(AR) Parkinsonism-dystonia, infantile, 1 (OMIM: 613135)	VUS	PM2, PP2, PP3

(*Continued on next page.*)

Table 3. (*Continued*)

Case	Study type	Gene	Chromosome (hg19)	HGVS DNA and protein reference	Zygosity	Parent of origin	Relevant disease association	Variant assessment	ACMG/AMP criteria met
25	Trio	*SRD5A2*	Chr 2:31758741 T > C	NM_000348.3 c.377A > G p.(Gln126Arg)	Het	Mat	(AR) Pseudovaginal perineoscrotal hypospadias (OMIM: 264600)	Pathogenic	PS3, PM2, PM3, PS4_Moderate, PP1, PP5
		SRD5A2	Chr 2:31758802 delG	NM_000348.3 c.317delC p.(Pro106LeufsTer25)	Het	Pat	(AR) Pseudovaginal perineoscrotal hypospadias (OMIM: 264600)	Likely pathogenic	PVS1, PM2
26	Trio	*TBCD*	Chr 17:80772747 G > A	NM_005993.4 c.1255G > A p.(Gly419Arg)	Het	Mat	(AR) Encephalopathy, progressive, early-onset, with brain atrophy and thin corpus callosum (OMIM: 617193)	VUS	PM2, PP3
		TBCD	Chr 17:80882859_ 80882861delGAG	NM_005993.4 c.2305_2307delGAG p.(Glu769del)	Het	Pat	(AR) Encephalopathy, progressive, early-onset, with brain atrophy and thin corpus callosum (OMIM: 617193)	VUS	PM2
27	Trio	*TRNT1*	Chr 3:3189583 C > G	NM_182916.2 c.1057-7C > G p.?	Het	Pat	(AR) Retinitis pigmentosa and erythrocytic microcytosis (OMIM: 616959) (AR) Sideroblastic anemia with B-cell immunodeficiency, periodic fevers, and developmental delay (OMIM: 616084)	Likely pathogenic	PM2, PM3, PP3, PP5
		TRNT1	Chr 3:3189779 A > G	NM_182916.2 c.1246A > G p.(Lys416Glu)	Het	Mat	(AR) Retinitis pigmentosa and erythrocytic microcytosis (OMIM: 616959); (AR) sideroblastic anemia with B-cell immunodeficiency, periodic fevers, and developmental delay (OMIM: 616084)	Likely pathogenic	PM2, PM3, PM_PS3
28	Trio	*UBA5*	Chr 3:132379541 dupA	NM_024818.3 c.160dupA p.(Ser54LysfsTer16)	Het	Mat	(AR) Epileptic encephalopathy, early infantile, 44 (OMIM: 617132)	Pathogenic	PVS1, PM1, PM2, PP3
		UBA5	Chr 3:132384835 G > A	NM_024818.3 c.215G > A p.(Arg72His)	Het	Pat	(AR) Epileptic encephalopathy, early infantile, 44 (OMIM: 617132)	Likely pathogenic	PM1, PM2, PM3, PP2
Autosomal recessive (one SNV + one copy loss)									
29	Trio	*IFT140*	Chr 16:1642177 C > T	NM_014714.3 c.634G > A p.(Gly212Arg)	Hemi (suspected deletion on other allele)	Mat	(AR) Short-rib thoracic dysplasia 9 with or without polydactyly (OMIM: 266920); (AR) Retinitis pigmentosa 80 (OMIM: 617781)	Pathogenic	PVS1, PS3, PM2, PM3, PP3, PP5
30	Trio	*NUBPL*	Chr 14:32319298 T > C	NM_025152.2 c.815-27T > C p.?	Hemi (~400kb deletion on other allele, by array)	Mat	(AR) Mitochondrial complex I deficiency, nuclear type 21 (OMIM: 618242)	Likely pathogenic	PS3, PP3, PP5; BS1
Autosomal dominant									
31	Trio	*ABCC9*	Chr 12:21995260 C > T	NM_020297.3 c.3461G > A p.(Arg1154Gln)	Het	De novo	(AD) Hypertrichotic osteochondrodysplasia (OMIM: 239850)	Pathogenic	PS1, PS2, PS3 PM2, PP2, PP3
32	Trio	*ANKRD11*	Chr 16:89345988 _89345989 insGGCTTCGG	NM_001256183.1 c.6968_6975dupCCCCGAAG p.(Ala2326ProfsTer14)	Het	De novo	(AD) KBG syndrome (OMIM: 148050)	Pathogenic	PVS1, PS2, PM2
33	Trio	*ANKRD11*	Chr 16:89349005delC	NM_001256182.1 c.3948delG p.(Leu1317Ter)	Het	De novo	(AD) KBG syndrome (OMIM: 148050)	Pathogenic	PVS1, PS2, PM2, PM4
34	Trio	*ANKRD11*	Chr 16:89351049_ 89351053delGTTTT	NM_001256182.1 c.1903_1907delAAACA p.(Lys635GlnfsTer26)	Het	De novo	(AD) KBG syndrome (OMIM: 148050)	Pathogenic	PVS1, PS2, PM2, PS4_Moderate, PP1, PP5

(*Continued on next page.*)

Table 3. (*Continued*)

Case	Study type	Gene	Chromosome (hg19)	HGVS DNA and protein reference	Zygosity	Parent of origin	Relevant disease association	Variant assessment	ACMG/AMP criteria met
35	Singleton	*ANKRD11*	Chr 16:89351049_89351053delGTTTT	NM_001256182.1 c.1903_1907delAAACA p.(Lys635GlnfsTer26)	Het	Unknown	(AD) KBG syndrome (OMIM: 148050)	Pathogenic	PVS1, PS2, PM2, PS4_Moderate, PP1, PP5
36	Trio	*ABCC9*	Chr 12:21995375 G > A	NM_005691.3 c.3346C > T p.(Arg1116Cys)	Het	Mat	(AD) Hypertrichotic osteochondrodysplasia (OMIM: 610253)	Likely pathogenic	PM2, PM5, PP2, PP3, PP5
37	Trio	*ACTB*	Chr 7:5568223 G > T	NM_001101.3 c.491C > A p.(Pro164His)	Het	De novo	(AD) ?Dystonia, juvenile-onset (OMIM: 607371); (AD) Baraitser–Winter syndrome 1 (OMIM: 243310)	Likely pathogenic	PS2, PM2, PP2, PP3
38	Trio	*ARID1B*	Chr 6:157528657 C > T	NM_020732.3 c.6382C > T p.(Arg2128Ter)	Het	De novo	(AD) Coffin–Siris syndrome 1 (OMIM: 135900)	Pathogenic	PVS1, PS2, PM2, PP5
39	Trio	*ATP6V1A*	Chr 3:113508666 G > A	NM_001690.3 c.967A > G p.(Arg323Gly)	Het	De novo	(AD) Epileptic encephalopathy, infantile or early childhood, 3 (OMIM: 618012)	Pathogenic	PS2, PM1, PM2, PP2, PP3
40	Trio	*CACNA1C*	Chr 12:2566837 T > C	NM_199460.3 c.722T > C p.(Val241Ala)	Het	De novo	(AD) Timothy syndrome (OMIM: 601005); (AD) Brugada syndrome 3 (OMIM: 611875)	Likely pathogenic	PS2, PM1, PM2, PP3
41	Trio	*CAMTA1*	Chr 1:7798409_7798411 delinsGTGCTGC	NM_015215.3 c.4049_4051delinsGTGCTGC p.(Pro1350ArgfsTer18)	Het	Mat	(AD) Cerebellar ataxia, nonprogressive, with mental retardation (OMIM: 614756)	Pathogenic	PVS1, PM2, PP1
42	Trio	*CAV3*	Chr 3:8787396 T > A	NM_001234.4 c.299T > A p.(Ile100Asn)	Het	De novo	(AD) Cardiomyopathy, familial hypertrophic (OMIM: 192600); (AD) creatine phosphokinase, elevated serum (OMIM: 123320); (AD) long QT syndrome 9 (OMIM: 611818); (AD) myopathy, distal, Tateyama type (OMIM: 614321); (AD) rippling muscle disease (OMIM: 606072)	Likely pathogenic	PS2, PM1, PM2, PP3
43	Trio	*CCND2*	Chr 12:4409144 C > A	NM_001759.3 c.839C > A p.(Thr280Asn)	Het	De novo	(AD) Megalencephaly-polymicrogyria-polydactyly-hydrocephalus syndrome 3 (OMIM: 615938)	Pathogenic	PS2, PM1, PM2, PS4_Moderate, PP5
44	Duo	*CHD2*	Chr 15:93485148 dupT	NM_001271.3 c.789dupT p.(Glu264Ter)	Het	Unknown	(AD) Epileptic encephalopathy, childhood-onset (OMIM: 615369)	Likely pathogenic	PVS1, PM2
45	Trio	*CHD7*	Chr 8:61773555_61773556 delAC	NM_017780.3 c.7701_7702delAC p.(Arg2568AspfsTer7)	Het	De novo	(AD) CHARGE syndrome (OMIM: 214800); (AD) hypogonadotropic hypogonadism 5 with or without anosmia (OMIM: 612370)	Pathogenic	PVS1, PS2, PM2
46	Singleton	*COL3A1*	Chr 2:189856222 G > T	NM_000090.3 c.862G > T p.(Gly288Cys)	Het	Unknown	(AD) Ehlers–Danlos syndrome, vascular type (OMIM: 130050)	Likely pathogenic	PM1, PM2, PP2, PP3
47	Trio	*CREBBP*	Chr 16:3779691 C > T	NM_004380.2 c.5357G > A p.(Arg1786His)	Het	De novo	(AD) Rubinstein–Taybi syndrome 1 (OMIM: 180849)	Likely pathogenic	PS2, PM1, PM2, PP3
48	Trio	*CREBBP*	Chr 16:3789597 C > A	NM_004380.2 c.4262G > T p.(Cys1421Phe)	Het	De novo	(AD) Rubinstein–Taybi syndrome 1 (OMIM: 180849)	Likely pathogenic	PS2, PM1, PM2, PP3
49	Trio	*CREBBP*	Chr 16:3842042 G > A	NM_004380.2 c.1270C > T p.(Arg424Ter)	Het	De novo	(AD) Rubinstein–Taybi syndrome 1 (OMIM: 180849)	Pathogenic	PVS1, PS2, PM2, PP5
50	Trio	*CSNK2A1*	Chr 20:476405 A > T	NM_177559.2 c.468T > A p.(Asp156Glu)	Het	De novo	(AD) Okur–Chung neurodevelopmental syndrome (OMIM: 617062)	Pathogenic	PS2, PM1, PM2, PM5, PP2, PP3, PP5

(*Continued on next page.*)

Table 3. (*Continued*)

Case	Study type	Gene	Chromosome (hg19)	HGVS DNA and protein reference	Zygosity	Parent of origin	Relevant disease association	Variant assessment	ACMG/AMP criteria met
51	Trio	*CSNK2A1*	Chr 20:485826 T > C	NM_177559.2 c.149A > G p.(Tyr50Cys)	Het	De novo	(AD) Okur–Chung neurodevelopmental syndrome (OMIM: 617062)	Pathogenic	PS2, PM2, PM5, PP2, PP5
52	Trio	*DYRK1A*	Chr 21:38862468_ 38862472 delCTCTT	NM_101395.2 c.665-9_665-5delCTCTT p.?	Het	De novo	(AD) Mental retardation, autosomal dominant 7 (OMIM: 614104)	Likely pathogenic	PS2, PM2, PP5
53	Singleton	*EFTUD2*	Chr 17:42964119 C > G	NM_004247.3 c.106-1G > C p.?	Het	Unknown	(AD) Mandibulofacial dysostosis, Guion–Almeida type (OMIM: 610536)	Pathogenic	PVS1, PM2, PP3
54	Duo	*EHMT1*	Chr 9:140637869 dupA	NM_024757.4 c.870dupA p.(Arg291ThrfsTer7)	Het	Unknown	(AD) Kleefstra syndrome 1 (OMIM: 610253)	Likely pathogenic	PVS1, PM2
55	Trio	*EHMT1*	Chr 9:140672394 dupC	NM_024757.4 c.2079dupC p.(Glu694ArgfsTer4)	Het	De novo	(AD) Kleefstra syndrome 1 (OMIM: 610253)	Pathogenic	PVS1, PS2, PM2
56	Trio	*FLG*[b]	Chr 1:152285861 G > A	NM_002016.1 c.1501C > T p.(Arg501Ter)	Het	Mat	(AD) Ichthyosis vulgaris (OMIM: 146700); (AD) {Dermatitis, atopic, susceptibility to, 2} (OMIM: 605803)	Pathogenic	PVS1, PM3, PP5
		FLG[b]	Chr 1:152285081_ 152285084delACGT	NM_002016.1 c.2282_2285delCAGT p.(Ser761CysfsTer36)	Het	Pat	(AD) Ichthyosis vulgaris (OMIM: 146700); (AD) {Dermatitis, atopic, susceptibility to, 2} (OMIM: 605803)	Pathogenic	PVS1, PS4, PM3, PP1
57	Trio	*FLG*[b]	Chr 1:152285861 G > A	NM_002016.1 c.1501C > T p.(Arg501Ter)	Het	Pat	(AD) Ichthyosis vulgaris (OMIM: 146700); (AD) {Dermatitis, atopic, susceptibility to, 2} (OMIM: 605803)	Pathogenic	PVS1, PS3, PP1, PP5
58	Trio	*FOXG1*	Chr 14:29237138 A > G	NM_005249.4 c.653A > G p.(Tyr218Cys)	Het	De novo	(AD) Rett syndrome, congenital variant (OMIM: 613454)	Likely pathogenic	PS2, PM2, PP3
59	Trio	*FOXP1*	Chr 3:71026799_ 71026802delTAAT	NM_001244810.1 c.1420_1423delATTA p.(Ile474GlyfsTer12)	Het	De novo	(AD) Mental retardation with language impairment and with or without autistic features (OMIM: 613670)	Pathogenic	PVS1, PS2, PM2
60	Duo	*GABRB2*	Chr 5:160758119 A > G	NM_021911.2 c.848T > C p.(Leu283Pro)	Het	Unknown	(AD) Epileptic encephalopathy, infantile or early childhood, 2 (OMIM: 617829)	VUS	PM1, PM2, PP3
61	Trio	*GABRB3*	Chr 15:27017618 T > A	NM_000814.5 c.173-2A > T p.?	Het	De novo	(AD) Epileptic encephalopathy, early infantile, 43 (OMIM: 617113)	Likely pathogenic	PS2, PM2, PP3
62	Trio	*GABRG2*	Chr 5:161569244 C > T	NM_198903.2 c.964C > T p.(Pro322Ser)	Het	De novo	(AD) Epilepsy, generalized, with febrile seizures plus, type 3 (OMIM: 607681); (AD) epileptic encephalopathy, early infantile, 74 (OMIM: 618396)	Pathogenic	PS2, PS3, PM2, PM5, PP2, PP3, PP5
63	Singleton	*HNRNPK*	Chr 9:86586597 dupT	NM_031263.3 c.998dupA p.(Tyr333Ter)	Het	Unknown	(AD) Au–Kline syndrome (OMIM: 616580)	Pathogenic	PVS1, PS2, PM2, PP5
64	Trio	*HRAS*	Chr 11:534289 C > T	NM_005343.2 c.34G > A p.(Gly12Ser)	Het	De novo	(AD) Costello syndrome (OMIM: 218040); (AD) Congenital myopathy with excess of muscle spindles (OMIM: 218040)	Pathogenic	PS2, PM1, PM2, PM5, PP5
65	Trio	*KANSL1*	Chr 17:44248468 G > A	NM_001193465.1 c.1042C > T p.(Arg348Ter)	Het	De novo	(AD) Koolen–De Vries syndrome (OMIM: 610443)	Pathogenic	PVS1, PS2, PM2, PP5
66	Singleton	*KMT2D*	Chr 12:49436599 G > A	NM_003482.3 c.5707C > T p.(Arg1903Ter)	Het	Unknown	(AD) Kabuki syndrome 1 (OMIM: 147920)	Pathogenic	PVS1, PM2, PM6, PP3, PP5

(*Continued on next page.*)

Table 3. (*Continued*)

Case	Study type	Gene	Chromosome (hg19)	HGVS DNA and protein reference	Zygosity	Parent of origin	Relevant disease association	Variant assessment	ACMG/AMP criteria met
67	Trio	*MED13L*	Chr 12:116452999_ 116453015 delTCTTTGGACTGTGCATC	NM_015335.4 c.1077_1093del p.(Met359IlefsTer38)	Het	De novo	(AD) Mental retardation and distinctive facial features with or without cardiac defects (OMIM: 616789); (AD) transposition of the great arteries, dextro-looped 1 (OMIM: 608808)	Pathogenic	PVS1, PS2, PM2
68	Trio	*MYT1L*	Chr 2:1915819 A > T	NM_015025.3 c.1676T > A p.(Val559Asp)	Het	De novo	(AD) Mental retardation, autosomal dominant 39 (OMIM: 616521)	Pathogenic	PS2, PM1, PM2, PP3, PP2
69	Trio	*MYT1L*	Chr 2:1906916 A > T	NM_001303052.1 c.1968T > A p.(Tyr656Ter)	Het	De novo	(AD) Mental retardation, autosomal dominant 39 (OMIM: 616521)	Pathogenic	PVS1, PS2, PM2
70	Trio	*NBEA*	Chr 13:35923346_ 35923347delAG	NM_015678.4 c.6005_6006delAG p.(Glu2002ValfsTer2)	Het	De novo	(AD) Seizures and intellectual disability (no OMIM) (PMID:28554332)	VUS	PM2, PS2_Moderate, PP3
71	Trio	*NEDD4L*	Chr 18:56033460 C > G	NM_001144967.2 c.2063C > G p.(Thr688Arg)	Het	Mat	(AD) Periventricular nodular heterotopia 7 (OMIM: 617201)	VUS	PM1, PM2, PP3
72	Trio	*NOTCH1*	Chr 9:139399384_ 139399385insTG	NM_017617.3 c.4758_4759insCA p.(Asn1587GlnfsTer30)	Het	Pat	(AD) Adams–Oliver syndrome 5 (OMIM: 616028); (AD) aortic valve disease 1 (OMIM: 109730)	Likely pathogenic	PVS1, PM2
73	Trio	*NSD2*	Chr 4:1906053 G > A	NM_133330.2 c.708G > A p.(Trp236Ter)	Het	De novo	(AD) Wolf–Hirchhorn syndrome–like (PMID: 31171569, 29884796)	Pathogenic	PVS1, PS2, PM2, PP3
74	Trio	*NSD2*	Chr 4:1936884dupG	NM_133330.2 c.1569dupG p.(Lys524GlufsTer17)	Het	De novo	(AD) Wolf–Hirchhorn syndrome–like (PMID: 31171569, 29884796)	Pathogenic	PVS1, PS2, PM2
75	Trio	*NSD2*	Chr 4:1918630 C > T	NM_133330.2 c.793C > T p.(Gln265Ter)	Het	De novo	(AD) Wolf–Hirchhorn syndrome–like (PMID: 31171569, 29884796)	Pathogenic	PVS1, PS2, PM2
76	Trio	*PPP2R5D*	Chr 6:42975698 A > C	NM_006245.3 c.752A > C p.(Asp251Ala)	Het	De novo	(AD) Mental retardation, autosomal dominant 35 (OMIM: 616355)	Pathogenic	PS2, PM2, PM5, PP2, PP3
77	Singleton	*PTPN11*	Chr 12:112888172 A > G	NM_002834.3 c.188A > G p.(Tyr63Cys)	Het	Unknown	(AD) Noonan syndrome 1 (OMIM: 163950); (AD) LEOPARD syndrome 1 (OMIM: 151100); (AD) metachondromatosis (OMIM: 156250)	Pathogenic	PS1, PS3, PS4, PP1_Strong, PM1, PP2, PP3
78	Trio	*PTPN11*	Chr 12:112915523 A > G	NM_002834.3 c.922A > G p.(Asn308Asp)	Het	De novo	(AD) Noonan syndrome 1 (OMIM: 163950); (AD) LEOPARD syndrome 1 (OMIM: 151100); (AD) metachondromatosis (OMIM: 156250)	Pathogenic	PS2_VERYStrong, PS3, PS4, PP1_Strong, PM1, PP2, PP3
79	Trio	*PUF60*	Chr 8:144898801 dupA	NM_078480.2 c.1569dupT p.(Glu524Ter)	Het	De novo	(AD) Verheij syndrome (OMIM: 615583)	Pathogenic	PVS1, PS2, PM2
80	Singleton	*RAI1*	Chr 17:17700943 C > T	NM_030665.3 c.4681C > T p.(Arg1561Ter)	Het	Unknown	(AD) Smith–Magenis syndrome (OMIM: 182290)	Pathogenic	PVS1, PM2, PP3
81	Trio	*SALL1*	Chr 16:51174260 C > A	NM_002968.2 c.1873G > T p.(Glu625Ter)	Het	Pat	(AD) Towne–Brocks syndrome 1 (OMIM: 107480)	Pathogenic	PVS1, PM2, PP1, PP3
82	Trio	*SATB2*	Chr 2:200193509 T > G	NM_015265.3 c.1298A > C p.(Tyr433Ser)	Het	De novo	(AD) Glass syndrome (OMIM: 612313)	Likely pathogenic	PS2, PM1, PM2, PP2
83	Trio	*SATB2*	Chr 2:200188564 delG	NM_015265.3 c.1504delC p.(Gln502LysfsTer44)	Het	De novo	(AD) Glass syndrome (OMIM: 612313)	Pathogenic	PVS1, PS2, PM1, PM2

(*Continued on next page.*)

Table 3. (*Continued*)

Case	Study type	Gene	Chromosome (hg19)	HGVS DNA and protein reference	Zygosity	Parent of origin	Relevant disease association	Variant assessment	ACMG/AMP criteria met
84	Trio	*SCN1A*	Chr 2:166850875 T > C	NM_001202435.1 c.4633A > G p.(Ile1545Val)	Het	De novo	(AD) Epilepsy, generalized, with febrile seizures plus, type 2 (OMIM: 604403); (AD) epileptic encephalopathy, early infantile, 6 (Dravet syndrome) (OMIM: 607208); (AD) febrile seizures, familial, 3A (OMIM: 604403); (AD) migraine, familial hemiplegic, 3 (OMIM: 609634)	Pathogenic	PS2, PM1, PM2, PP2, PP3
85	Trio	*SCN8A*	Chr 12:52159459 G > A	NM_014191.3 c.2549G > A p.(Arg850Gln)	Het	De novo	(AD) Cognitive impairment with or without cerebellar ataxia (OMIM: 614306); (AD) epileptic encephalopathy, early infantile, 13 (OMIM: 614558); (AD) seizures, benign familial infantile, 5 (OMIM: 617080)	Pathogenic	PS2, PM1, PM2, PP2, PP3, PP5
86	Duo	*SERPINC1*	Chr 1:173879999 T > C	NM_000488.3 c.655A > G p.(Asn219Asp)	Het	Mat	(AD,AR) Thrombophilia due to antithrombin III deficiency (OMIM: 613118)	Likely pathogenic	PM2, PM5, PS4_Moderate, PP2, PP3
87	Trio	*SETD5*	Chr 3:9483407 A > G	NM_001292043.1 c.647A > G p.(Asn216Ser)	Het	De novo	(AD) Mental retardation, autosomal dominant 23 (OMIM: 615761)	Likely pathogenic	PS2, PM2, PP3, BP1
88	Trio	*SHANK3*	Chr 22:51160025_51160037 delGGGCCCAGCCCCC	NM_033517.1 c.3764_3776del p.(Arg1255LeufsTer25)	Het	De novo	(AD) Phelan–McDermid syndrome (OMIM: 606232)	Pathogenic	PVS1, PS2, PM2
89	Trio	*SLC2A1*	Chr 1:43394689 G > A	NM_006516.2 c.988C > T p.(Arg330Ter)	Het	De novo	(AD,AR) GLUT1 deficiency syndrome 1, infantile onset, severe (OMIM: 606777); (AD) GLUT1 deficiency syndrome 2, childhood onset (OMIM: 612126); (AD) dystonia 9 (OMIM: 601042); (AD) Stomatin-deficient cryohydrocytosis with neurologic defects (OMIM: 608885)	Pathogenic	PVS1, PS2, PM2, PP3, PP5
90	Trio	*SLC2A1*	Chr 1:43394649 dupC	NM_006516.2 c.1028dupG p.(Met344HisfsTer37)	Het	De novo	(AD,AR) GLUT1 deficiency syndrome 1, infantile onset, severe (OMIM: 606777); (AD) GLUT1 deficiency syndrome 2, childhood onset (OMIM: 612126); (AD) dystonia 9 (OMIM: 601042); (AD) Stomatin-deficient cryohydrocytosis with neurologic defects (OMIM: 608885)	Pathogenic	PVS1, PS2, PM2
91	Trio	*SMAD4*	Chr 18:48604676 A > G	NM_005359.5 c.1498A > G p.(Ile500Val)	Het	De novo	(AD) Myhre syndrome (OMIM: 139210); (AD) juvenile polyposis/hereditary hemorrhagic telangiectasia syndrome (OMIM: 175050); (AD) polyposis, juvenile intestinal (OMIM: 174900)	Pathogenic	PS2, PS3, PM1, PM2, PM5, PP2, PP3, PP5
92	Trio	*SON*	Chr 21:34929623 G > A	NM_138927.3 c.6321 + 1G > A p.?	Het	De novo	(AD) ZTTK syndrome (OMIM: 617140)	Pathogenic	PVS1, PS2, PM2
93	Trio	*STXBP1*	Chr 9:130440731_130440740dup AAGCCGGAGC	NM_003165.3 c.1381_1390 dupAAGCCGGAGC p.(Arg464GlnfsTer31)	Het	De novo	(AD) Epileptic encephalopathy, early infantile, 4 (OMIM: 612164)	Pathogenic	PVS1, PS2, PM2

(*Continued on next page.*)

Table 3. (*Continued*)

Case	Study type	Gene	Chromosome (hg19)	HGVS DNA and protein reference	Zygosity	Parent of origin	Relevant disease association	Variant assessment	ACMG/AMP criteria met
94	Trio	*STXBP1*	Chr 9:130440777 C > G	NM_003165.3 c.1427C > G p.(Ser476Ter)	Het	De novo	(AD) Epileptic encephalopathy, early infantile, 4 (OMIM: 612164)	Pathogenic	PVS1, PS2, PM2
95	Duo	*SYNGAP1*	Chr 6:33411735 C > T	NM_006772.2 c.3406C > T p.(Gln1136Ter)	Het	Unknown	(AD) Mental retardation, autosomal dominant 5 (OMIM: 612621)	Likely pathogenic	PVS1, PM2
96	Trio	*TBL1XR1*	Chr 3:176767798 G > A	NM_024665.4 c.689C > T p.(Ser230Phe)	Het	De novo	(AD) Mental retardation, autosomal dominant 41 (OMIM: 616944) (AD) Pierpont syndrome (OMIM: 602342)	Likely pathogenic	PS2, PM2, PP2, PP3
97	Trio	*TBX1*	Chr 22:19750829 T > C	NM_005992.1 c.476T > C p.(Leu159Pro)	Het	De novo	(AD) DiGeorge syndrome (OMIM: 188400); (AD) tetralogy of Fallot (OMIM: 187500); (AD) velocardiofacial syndrome (OMIM: 192430)	Likely pathogenic	PS2, PM2, PP3
98	Trio	*TCF4*	Chr 18:52921925 G > A	NM_001243226.2 c.1459C > T p.(Arg487Ter)	Het	De novo	(AD) Corneal dystrophy, Fuchs endothelial, 3 (OMIM: 613267); (AD) Pitt–Hopkins syndrome (OMIM: 610954)	Pathogenic	PVS1, PS2, PS3, PM2, PS4_Moderate
99	Duo	*TUBB4A*	Chr 19:6495765 C > T	NM_001289123.1 c.898G > A p.(Asp300Asn)	Het	Unknown	(AD) Dystonia 4, torsion, autosomal dominant (OMIM: 128101); (AD) leukodystrophy, hypomyelinating, 6 (OMIM: 612438)	Pathogenic	PS2, PS3, PM1, PM2, PP2, PP3
100	Trio	*ZEB2*	Chr 2:145156329 C > A	NM_014795.3 c.2425G > T p.(Glu809Ter)	Het	De novo	(AD) Mowat–Wilson syndrome (OMIM: 235730)	Pathogenic	PVS1, PS2, PM2, PP3
101	Trio	*ZEB2*	Chr 2:145157206_145157213 delCACTACCG	NM_014795.3 c.1541_1548delCGGTAGTG p.(Pro514GlnfsTer3)	Het	De novo	(AD) Mowat-Wilson syndrome (OMIM: 235730)	Pathogenic	PVS1, PS2, PM2
X-linked									
102	Trio	*DDX3X*	Chr X:41203603 C > T	NM_001356.4 c.976C > T p.(Arg326Cys)	Het	De novo	(XLD,XLR) Mental retardation, X-linked 102 (OMIM: 300958)	Pathogenic	PS2, PM1, PM2, PM5, PP2, PP3
103	Singleton	*DDX3X*	Chr X:41205795_ 41205796delAT	NM_001356.4 c.1535_1536delAT p.(His512ArgfsTer5)	Het	Unknown	(XLD,XLR) Mental retardation, X-linked 102 (OMIM: 300958)	Pathogenic	PVS1, PM1, PM2, PM6, PS4_Moderate
104	Trio	*IQSEC2*	Chr X:53263455 delG	NM_001111125.2 c.4419delC p.(Ser1474ValfsTer21)	Het	De novo	(XLD) Mental retardation, X-linked 1/78 (OMIM: 309530)	Pathogenic	PVS1, PS2
105	Trio	*IQSEC2*	Chr X:53277294 A > G	NM_001111125.2 c.2582 + 2T > C p.?	Het	De novo	(XLD) Mental retardation, X-linked 1/78 (OMIM: 309530)	Pathogenic	PVS1, PS2, PM2
106	Trio	*IQSEC2*	Chr X:53277371 G > A	NM_001111125.2 c.2507C > T p.(Ala836Val)	Het	Unknown	(XLD) Mental retardation, X-linked 1/78 (OMIM: 309530)	Likely pathogenic	PS2, PM2, PS4_Moderate, PP3
107	Trio	*KDM5C*	Chr X:53223464 C > A	NM_004187.3 c.3895G > T p.(Glu1299Ter)	Het	De novo	(XLR) Mental retardation, X-linked, syndromic, Claes–Jensen type (OMIM: 300534)	Pathogenic	PVS1, PS2, PM2
108	Trio	*MECP2*	Chr X:153296860 G > A	NM_004992.3 c.419C > T p.(Ala140Val)	Hemi	Mat	(XLR) Mental retardation, X-linked, syndromic 13 (OMIM: 300055); (XLR) encephalopathy, neonatal severe (OMIM: 300673); (XLR) mental retardation, X-linked syndromic, Lubs type (OMIM: 300260); (XLD) Rett syndrome (OMIM: 312750) (XL) {Autism susceptibility, X-linked 3} (OMIM: 300496)	Pathogenic	PS3, PM1, PM2, PS4_Moderate, PP1, PP3, PP5

(*Continued on next page.*)

Table 3. (*Continued*)

Case	Study type	Gene	Chromosome (hg19)	HGVS DNA and protein reference	Zygosity	Parent of origin	Relevant disease association	Variant assessment	ACMG/AMP criteria met
109	Trio	*MED12*	Chr X:70349963 C > G	NM_005120.2 c.3946C > G p.(Gln1316Glu)	Hemi	Mat	(XLR) Opitz–Kaveggia syndrome (OMIM: 305450); (XLR) Lujan–Fryns syndrome (OMIM: 309520); (XLR) Ohdo syndrome, X-linked (OMIM: 300895)	VUS	PM2, PP3
110	Trio	*NAA10*	Chr X:153197853 A > C	NM_003491.3 c.257T > G p.(Leu86Arg)	Het	De novo	(XL) ?Microphthalmia, syndromic 1 (OMIM: 309800); (XLD,XLR) Ogden syndrome (OMIM: 300855)	Pathogenic	PS2, PM1, PM2, PP2, PP3
111	Trio	*PIGA*	Chr X:15339728 T > A	NM_002641.3 c.1355A > T p.(Asp452Val)	Hemi	De novo	(XLR) Multiple congenital anomalies-hypotonia-seizures syndrome 2 (OMIM: 300868); (XLR) paroxysmal nocturnal hemoglobinuria, somatic (OMIM: 300818)	Likely pathogenic	PS2, PM2, PP3
112	Duo	*PIGA*	Chr X:15349685 G > A	NM_002641.3 c.368C > T p.(Thr123Met)	Hemi	Mat	(XLR) Multiple congenital anomalies-hypotonia-seizures syndrome 2 (OMIM: 300868) (XLR) Paroxysmal nocturnal hemoglobinuria, somatic (OMIM: 300818)	Likely pathogenic	PM1, PM2, PP3, PP5
113	Trio	*RPS6KA3*	Chr X:20213249 G > A	NM_004586.2 c.340C > T p.(Arg114Trp)	Hemi	Mat	(XLD) Coffin–Lowry syndrome (OMIM: 303600)	Likely pathogenic	PM1, PM2, PS4_Moderate, PP1, PP2, PP3
114	Trio	*RPS6KA3*	Chr X:20179827 G > A	NM_004586.2 c.1894C > T p.(Arg632Ter)	Hemi	De novo	(XLD) Coffin–Lowry syndrome (OMIM: 303600)	Pathogenic	PVS1, PS2, PM2, PP5
115	Trio	*SMC1A*	Chr X:53410095 dupT	NM_001281463.1 c.3053dupA p.(Arg1019AlafsTer26)	Het	Unknown	(XLD) Cornelia de Lange syndrome 2 (OMIM: 300590)	Pathogenic	PVS1, PM2

(HGVS) Human Genome Variation Society, (ACMG/AMP) American College of Medical Genetics and Genomics/Association for Molecular Pathology, (hemi) hemizygous, (het) heterozygous, (hom) homozygous, (mat) maternal, (pat) paternal, (AR) autosomal recessive, (AD) autosomal dominant, (XL) X-linked, (XLD) X-linked dominant, (XLR) X-linked recessive, (VUS) variant of uncertain significance.

[a]Proband with two disorders.

[b]Semidominant.

Among the 115 provider-substantiated diagnostic cases with 117 disorders, a causal variant with a VAF < 20% (Supplemental Table 1) occurred in five probands and contributed to 4.3% [95% CI, 1.4%–9.9%] of our total diagnoses and 7.9% [95% CI, 2.6%–17.6%] of our confirmed de novo variants. As established within our pipeline, heterozygous calls (0/1 genotype) rarely deviate toward extreme allelic proportions, with 0.3% of high-confidence calls within a reference standard occurring at VAF < 20 or VAF > 80 (Supplemental Fig. 1). In addition, causal variants in two probands were found in a mosaic state in two unaffected parents (0.3% of available parental samples). All mosaic variants were verified by Sanger sequencing analysis as evidenced by disparate peak height in the electropherogram (Supplemental Fig. 2). In total, mosaic etiology in a proband, or that originating in a parent with transmission to a proband, was associated with seven out of 117 (6.0%) provider-substantiated genetic diagnoses. These mosaic variants were recurrently associated with several types of disorders, predominately involving neurodevelopmental features, including early infantile epileptic encephalopathies, intellectual disability syndromes, Coffin–Siris syndrome, and megalencephaly-polymicrogyria-polydactyly-hydrocephalus syndrome (MPPH) (Table 3).

DISCUSSION

We evaluated the concordance of the molecular ES diagnostic rate generated by the clinical laboratory with ordering clinical provider-substantiated diagnoses. Our results demonstrate the robust clinical utility of ES, with 91.4% of the laboratory findings reported as likely causal for the proband phenotype resulting in a clinically confirmed diagnosis by the ordering provider. This concordance may increase over time, as four laboratory-reported diagnostic cases were still under consideration in the patient differential. The high concordance rate may be attributable to the detailed clinical feature information form submitted by an experienced clinical geneticist or genetic counselor at the time of ES ordering, additional curation of the medical record as performed by the variant analysis team or laboratory genetic counselor to enable a phenotype-informed variant analysis approach, and the multidisciplinary expertise achieved by group evaluation of annotated, filtered variants in a case conference setting. Within our primarily pediatric population, we obtained a 32.2% diagnostic yield, with 64.9% of causal variants identified by trio analysis confirmed as de novo. These numbers are in line with previously reported exome and genome sequencing diagnostic yields (average = 31%) and de novo rates (average = 44%) (Clark et al. 2018). In comparison to other large clinical exome sequencing cohorts, our study found a similar rate of cases submitted for trio analysis. In addition, the distribution of AD, AR, and XL inheritance patterns of causal variants were also comparable (Yang et al. 2013, 2014; Lee et al. 2014; Farwell et al. 2015; Retterer et al. 2016).

Of the 115 diagnostic cases, we confirmed mosaicism of a disease-associated variant in five probands and two parental samples. The contribution of parental mosaicism may be higher, given that trio analyses were available for 74.8% of our cases. The frequency of mosaicism in our cohort is higher than what has previously been reported in unselected clinical exome sequencing cohorts (Yang et al. 2013; Retterer et al. 2016; Cao et al. 2019). Several differences between our study and previous reports may contribute to this difference, including sequencing in a hospital-based laboratory representing a pediatric patient population referred by clinical geneticists within a single institution, stringent quality control metrics for sequencing data (including both assay and variant quality measures), diagnostic yield based on EMR clinical substantiation versus solely a laboratory-defined molecular diagnostic yield, and manual evaluation of all assessed variants with specific review of aligned reads and variant characteristics in proband and parental samples.

Our positive mosaic findings contributed to several types of disorders associated with neurodevelopmental features including Coffin–Siris syndrome ($n = 2$), early infantile epileptic encephalopathy ($n = 2$), intellectual disability syndromes ($n = 2$), and the brain overgrowth syndrome MPPH ($n = 1$). The presence of mosaicism in these patients is consistent with the reported association of mosaic variants within these types of disorders (Krupp et al. 2017; Lim et al. 2017; Madsen et al. 2018; Stosser et al. 2018). The enrichment of our pediatric ES population for various neurodevelopmental features, such as developmental delays, cognitive impairment, and autistic behavior, also may have contributed to the high prevalence of mosaicism seen within this cohort.

Identifying that a disease-causing variant is mosaic can have several implications when counseling families. Although the presence of mosaicism is generally unable to predict disease severity, as often only a single tissue type is available for study, it can be informative in providing a clinical explanation for a proband with a mild presentation. In this cohort, detection of mosaicism provided a mechanism to explain a mildly affected male diagnosed with the X-linked disorder, early infantile epileptic encephalopathy 2, primarily seen in females (Case 2). Identifying mosaicism in proband or parental samples is of particular importance to inform recurrence risk in future pregnancies. Evaluating parental samples for the presence of mosaicism can also be beneficial for providing an explanation for why a parent positive for pathogenic variant may be mildly symptomatic or unaffected, as evidenced in this series by the unaffected mother with an *IQSEC2* mosaic variant, which was hemizygous in the affected proband, as well as his affected brother (Case 4, previously reported by Barrie et al. 2019).

Mosaic variants can be challenging to detect clinically because of several factors, and consensus guidelines addressing how to detect, assess, and report mosaicism are not currently available. These variants can occur at very low frequencies and thus may be below the threshold of detection if coverage or read depth is insufficient at the affected residue. Acuna-Hidalgo et al. (2015) modeled that the probability of detecting mosaicism at 100× coverage is >90% for variants occurring at 10% VAF or higher. However, the ability to detect these variants decreases considerably with decreasing read depth. The higher sequence depth in coding regions typically achieved by exome sequencing thus offers an advantage for detecting mosaicism compared to genome sequencing, because of cost-related limitations to genome sequencing read depth. Despite sufficient coverage across a given region, if the variant is present in a limited number of reads, it may be below the sensitivity of the variant caller software. In our cohort, one of the mosaic variants in a parental sample (Case 6), the *ARID2* variant at 4% VAF, was not detected by the variant caller and came to attention during manual review of reportable variants within aligned sequencing reads. This highlights the utility in manual review of variant calls within the aligned reads to evaluate variant authenticity.

Alternatively, identifying an authentic mosaic variant can also present a challenge. With MPS, false-positive variants may occur by several means. These include biologic contamination during sample acquisition, nucleic acid extraction, or library preparation, low-level admixture during sequencing, or as a result of sample carryover from prior sequencing runs, as well as polymerase chain reaction (PCR) or sequencing artifacts (incorporation errors and library chimeras). Additionally, index hopping can result in false positive calls at very low-level as single-indexed reads can incur misassignment of indices within multiplexed libraries, a phenomenon known to be enhanced on patterned flow cells in short-read sequencing chemistries. The confounding variable of index hopping in the setting of trio analyses can be decreased by the use of dual indexing of libraries (Costello et al. 2018). To increase confidence in calling mosaicism and rare, low-frequency variants, the addition of dual-indexed libraries containing unique identifiers known as molecular barcodes (Kinde et al. 2011; Schmitt et al. 2012) allows discrimination of improperly indexed libraries and random errors. In this study, all de novo and mosaic variants called with single-indexed

libraries were confirmed by Sanger sequencing. Evidence of the low-level variant allele could be visualized for all mosaic variants by review of peak heights in the electropherogram. A priori knowledge of suspected mosaicism facilitated review of Sanger sequencing data and enabled scrutiny of allelic peak heights, including the variant allele relative to background. Thus, data points from two orthogonal methodologies (MPS and Sanger) were considered prior to report out of a mosaic call. The variant with a VAF of 4% in a maternal sample (Case 6) was visualized by Sanger sequencing, despite being below the threshold typically appreciable by this method (~10%–20%), because of the nature of the variant (2-nt deletion), as well as prior observation of the heterozygous variant in the proband. However, if the VAF is too low to be appreciable by Sanger, high-depth amplicon sequencing or other quantitative approaches including digital droplet PCR could be used. The testing of alternative tissue sources can also be considered to aid in confirming suspected mosaicism in patients, although multiple tissue sources may be required, and may be impractical or impossible to obtain. Authentic mosaic variants with high VAFs can also be challenging to detect, as they may be mistaken for heterozygous calls that deviate from the expected 50% VAF because of technical variation and platform bias (Acuna-Hidalgo et al. 2015).

Outside of technical limitations of the assay, mosaic variants can go undetected when the variant is confined to specific tissue types. In these cases, sequencing of the affected tissues is required for detection. Confinement of mosaicism in a parent to predominately or exclusively germline cells would also go undetected by clinical ES trio analysis and typically only comes to light in instances of multiple affected children from an otherwise unaffected parent.

In conclusion, our study highlights two years of an ongoing ES assay within a pediatric tertiary care institution and emphasizes the utility of clinical-provider engagement in ES test ordering and phenotypic curation, as demonstrated by the strong concordance of laboratory-reported and ordering provider-substantiated diagnostic yield. Additionally, we demonstrate that mosaicism is an important contributor to disease-causing variation identified by ES within the pediatric population. Given that our diagnostic yield of mosaic variants exceeds those reported by other ES studies, vigilant manual review of variant calls by a highly skilled variant analysis team and clinical laboratory directors may be a key differentiator in detecting somatic mosaic events. This must occur in concert with adequate read depth and breadth of the assay, appropriate bioinformatic processing parameters, and in consideration of the proband's clinical characteristics to attribute causality. As we begin to appreciate the expanding role of mosaicism in genetic disease, further research on the types of disorders with mosaicism, clinical implications, and optimal laboratory practices for identifying and reporting mosaicism are needed.

METHODS

Sequencing, Bioinformatics, and Quality Control

Proband and parental peripheral blood samples were submitted for ES to The Steve and Cindy Rasmussen Institute for Genomic Medicine at Nationwide Children's Hospital, Columbus, Ohio. Prior to ES studies, microarray analysis was previously performed on the submitted proband, unless deemed to not be clinically indicated by the ordering provider (5% of the cohort). Genomic DNA was extracted using the Puregene DNA isolation kit according to the manufacturer protocol (QIAGEN) or EZ1 DNA isolation kit (QIAGEN), with two separate DNA extractions performed per each submitted proband and parental sample to facilitate identity and provenance analyses. Genotyping of 30 autosomal loci representing single-nucleotide variants with high population minor allele frequency was performed in the parental and proband samples using a custom Agena MassArray panel (Agena). Subsequently, a comparison of the Agena-derived genotype data was performed relative

to aligned sequencing read data derived by MPS to further ensure sample provenance throughout the extraction, library preparation, sequencing, and bioinformatic analysis stages, as well as to verify familial relationships.

Libraries were subject to target capture using SureSelect Human All Exon V6 (Agilent) followed by paired-end 101- or 151-bp sequencing to 137× mean depth on a HiSeq 2500 or HiSeq 4000 (Illumina), with 96.5% of targeted bases at 20× or greater (Supplemental Table 2). Sequencing data were demultiplexed and analyzed by GenomeNext (Columbus, OH) v1.1, which performs alignment to the reference sequence (GRCh37/hg19 Feb 2009), deduplication, and single sample variant calling with GATK Unified Genotyper 1.6–13 via the Churchill secondary analysis pipeline (Kelly et al. 2015). Mitogen (Sunquest) was used for annotation and tertiary analysis filtering informed by clinician-provided phenotypes, which were converted into HPO terms (Kohler et al. 2017).

As standard of practice in our exome workflow, aligned sequencing reads in the BAM file were reviewed at all assessed variants using the Integrative Genomics Viewer v2.3-2.4.4 (Broad) (Robinson et al. 2011). This allowed for a review of variant authenticity and encompassed an examination of read counts and strandedness, location of the variant within the read, VAF, homology, read quality, and mapping. Manual review of read-aligned proband data was performed relative to review of identity-confirmed parental sequence to allow for side-by-side comparison, with IGV alignment preferences set to allow for display of coverage allele-fraction threshold at 2% and retention of soft-clipped reads. Genomic regions with known homology as defined by Mandelker et al. (2016) have been incorporated into ES analysis through BED file track definitions to visually flag the level of homology of the local region in IGV. Parentage was confirmed in our data set for all de novo calls, with familial relationships established by genotyping per our standard workflow. Hemizygous variants were X-linked variants identified in >95% of reads in male patients. Homozygous calls applied to autosomal variants in >95% of reads. Variants deviating to the extreme of VAF <20 or >80 were considered suspicious for mosaicism, and subsequently underwent orthogonal testing by Sanger sequencing.

Sanger sequencing was performed on proband and available parental samples for all de novo variants and suspected mosaic variants identified as likely causal for the proband phenotype. Analysis by Sanger was used to distinguish from MPS or PCR artifact, and verify reduction in allelic ratio as visualized by disparate peak heights for mosaicism. For Sanger sequencing, PCR amplification of the region of interest was followed by purification using the QIAquick purification kit (QIAGEN). Forward and reverse sequencing reactions were performed with the Big Dye v3.1 terminator mix (ThermoFisher). Sequencing was performed on an Applied Biosystems 3130 or 3730 instrument (ThermoFisher). Mosaic variants were confirmed by observation of a nonreference allele with a disparate peak height during Sanger analysis.

Variant Interpretation

Custom scripting allowed for enrichment of variant attribute data including disease association and phenotype overlap. For each proband, the annotated filtered variant list was evaluated at a case conference attended by laboratory directors, genetic counselors, variant scientists, residents, fellows, and geneticists, including the ordering provider, when available. Variants that met group consensus were assessed according to ACMG/AMP recommendations (Richards et al. 2015). Following assessment, variants are reported as either likely causal for proband phenotype or as findings of undetermined clinical relevance to the proband phenotype based upon strength of phenotype overlap with the associated disease at the discretion of the ABMGG board-certified signing director. Laboratory diagnostic yield was defined as the number of cases with a variant or variants reported as likely causal for

the proband phenotype. Concordance between the laboratory and the ordering provider as to reported variant-associated disease causality was examined via clinical documentation in the EMR. Variants were considered clinically confirmed as causal if the ordering provider attributed some or all features in the proband to the variant(s).

ADDITIONAL INFORMATION

Data Deposition and Access

The mosaic variants were submitted to ClinVar (http://www.ncbi.nlm.nih.gov/clinvar/) under accession numbers SCV001161761.1, SCV001161762.1, SCV001161763.1, SCV000864353.2, SCV001161764.1, SCV001161765.1, and SCV001161766.1. Additional variants from the 117 diagnostic cases have been deposited to ClinVar under submitter Institute for Genomic Medicine (IGM) Clinical Laboratory, Nationwide Children's Hospital. Details are provided in the supplemental material. Deposition of raw sequencing data is not permitted based on patient consent.

Ethics Statement

All patients or their guardians provided written informed consent for genomic sequencing. This research is under a protocol approved by the Institutional Review Board at Nationwide Children's Hospital (IRB18-00662).

Competing Interest Statement

The authors have declared no competing interest.

Referees

Tomi Pastinen
Anonymous

Received February 15, 2020; accepted in revised form April 29, 2020.

Acknowledgments

We thank the patients, families, and clinicians involved in these cases. We acknowledge Maria Alfaro, PhD, Erik Zmuda, PhD, and Julie Gastier-Foster, PhD for their contributions in clinical patient care.

Author Contributions

C.R.M. prepared the manuscript. All authors contributed to design of workflows and data procurement and reviewed and approved the manuscript. C.E.C. supervised the study.

REFERENCES

Acuna-Hidalgo R, Bo T, Kwint MP, van de Vorst M, Pinelli M, Veltman JA, Hoischen A, Vissers LE, Gilissen C. 2015. Post-zygotic point mutations are an underrecognized source of de novo genomic variation. *Am J Hum Genet* **97:** 67–74. doi:10.1016/j.ajhg.2015.05.008

Aldred MA, Trembath RC. 2000. Activating and inactivating mutations in the human *GNAS1* gene. *Hum Mutat* **16:** 183–189. doi:10.1002/1098-1004(200009)16:3<183::AID-HUMU1>3.0.CO;2-L

Bahi-Buisson N, Villeneuve N, Caietta E, Jacquette A, Maurey H, Matthijs G, Van Esch H, Delahaye A, Moncla A, Milh M, et al. 2012. Recurrent mutations in the *CDKL5* gene: genotype–phenotype relationships. *Am J Med Genet* **158A:** 1612–1619. doi:10.1002/ajmg.a.35401

Barrie ES, Cottrell CE, Gastier-Foster J, Hickey SE, Patel AD, Santoro SL, Alfaro MP. 2019. Genotype-phenotype correlation: inheritance and variant-type infer pathogenicity in *IQSEC2* gene. *Eur J Med Genet* **12:** 103735. doi:10.1016/j.ejmg.2019.103735

Biesecker LG, Spinner NB. 2013. A genomic view of mosaicism and human disease. *Nat Rev Genet* **14:** 307–320. doi:10.1038/nrg3424

Bogershausen N, Wollnik B. 2018. Mutational landscapes and phenotypic spectrum of SWI/SNF-related intellectual disability disorders. *Front Mol Neurosci* **11:** 252. doi:10.3389/fnmol.2018.00252

Bramswig NC, Lüdecke HJ, Pettersson M, Albrecht B, Bernier RA, Cremer K, Eichler EE, Falkenstein D, Gerdts J, Jansen S, et al. 2017a. Identification of new *TRIP12* variants and detailed clinical evaluation of individuals

with non-syndromic intellectual disability with or without autism. *Hum Genet* **136:** 179–192. doi:10.1007/s00439-016-1743-x

Bramswig NC, Caluseriu O, Lüdecke HJ, Bolduc FV, Noel NC, Wieland T, Surowy HM, Christen HJ, Engels H, Strom TM, et al. 2017b. Heterozygosity for *ARID2* loss-of-function mutations in individuals with a Coffin–Siris syndrome-like phenotype. *Hum Genet* **136:** 297–305. doi:10.1007/s00439-017-1757-z

Cao Y, Tokita MJ, Chen ES, Ghosh R, Chen T, Feng Y, Gorman E, Gibellini F, Ward PA, Braxton A, et al. 2019. A clinical survey of mosaic single nucleotide variants in disease-causing genes detected by exome sequencing. *Genome Med* **11:** 48. doi:10.1186/s13073-019-0658-2

Clark MM, Stark Z, Farnaes L, Tan TY, White SM, Dimmock D, Kingsmore SF. 2018. Meta-analysis of the diagnostic and clinical utility of genome and exome sequencing and chromosomal microarray in children with suspected genetic diseases. *NPJ Genom Med* **3:** 16. doi:10.1038/s41525-018-0053-8

Costello M, Fleharty M, Abreu J, Farjoun Y, Ferriera S, Holmes L, Granger B, Green L, Howd T, Mason T, et al. 2018. Characterization and remediation of sample index swaps by non-redundant dual indexing on massively parallel sequencing platforms. *BMC Genomics* **19:** 332. doi:10.1186/s12864-018-4703-0

Ewans LJ, Field M, Zhu Y, Turner G, Leffler M, Dinger ME, Cowley MJ, Buckley MF, Scheffer IE, Jackson MR, et al. 2017. Gonadal mosaicism of a novel *IQSEC2* variant causing female limited intellectual disability and epilepsy. *Eur J Hum Genet* **25:** 763–767. doi:10.1038/ejhg.2017.29

Ewans LJ, Schofield D, Shrestha R, Zhu Y, Gayevskiy V, Ying K, Walsh C, Lee E, Kirk EP, Colley A, et al. 2018. Whole-exome sequencing reanalysis at 12 months boosts diagnosis and is cost-effective when applied early in Mendelian disorders. *Genet Med* **20:** 1564–1574. doi:10.1038/gim.2018.39

Farwell KD, Shahmirzadi L, El-Khechen D, Powis Z, Chao EC, Tippin Davis B, Baxter RM, Zeng W, Mroske C, Parra MC, et al. 2015. Enhanced utility of family-centered diagnostic exome sequencing with inheritance model-based analysis: results from 500 unselected families with undiagnosed genetic conditions. *Genet Med* **17:** 578–586. doi:10.1038/gim.2014.154

Gronskov K, Diness B, Stahlhut M, Zilmer M, Tumer Z, Bisgaard AM, Brondum-Nielsen K. 2014. Mosaicism for c.431_454dup in *ARX* causes a mild Partington syndrome phenotype. *Eur J Med Genet* **57:** 284–287. doi:10.1016/j.ejmg.2014.03.009

Hu X, Li N, Xu Y, Li G, Yu T, Yao RE, Fu L, Wang J, Yin L, Yin Y, et al. 2018. Proband-only medical exome sequencing as a cost-effective first-tier genetic diagnostic test for patients without prior molecular tests and clinical diagnosis in a developing country: the China experience. *Genet Med* **20:** 1045–1053. doi:10.1038/gim.2017.195

Hucthagowder V, Shenoy A, Corliss M, Vigh-Conrad KA, Storer C, Grange DK, Cottrell CE. 2016. Utility of clinical high-depth next generation sequencing for somatic variant detection in the *PIK3CA*-related overgrowth spectrum. *Clin Genet* **91:** 79–85. doi:10.1111/cge.12819

Kelly BJ, Fitch JR, Hu Y, Corsmeier DJ, Zhong H, Wetzel AN, Nordquist RD, Newsom DL, White P. 2015. Churchill: an ultra-fast, deterministic, highly scalable and balanced parallelization strategy for the discovery of human genetic variation in clinical and population-scale genomics. *Genome Biol* **16:** 6. doi:10.1186/s13059-014-0577-x

Keppler-Noreuil KM, Rios JJ, Parker VE, Semple RK, Lindhurst MJ, Sapp JC, Alomari A, Ezaki M, Dobyns W, Biesecker LG. 2015. *PIK3CA*-related overgrowth spectrum (PROS): diagnostic and testing eligibility criteria, differential diagnosis, and evaluation. *Am J Med Genet* **167:** 287–295. doi:10.1002/ajmg.a.36836

Kilstrup-Nielsen C, Rusconi L, La Montanara P, Ciceri D, Bergo A, Bedogni F, Landsberger N. 2012. What we know and would like to know about CDKL5 and its involvement in epileptic encephalopathy. *Neural Plast* **2012:** 728267. doi:10.1155/2012/728267

Kinde I, Wu J, Papadopoulos N, Kinzler KW, Vogelstein B. 2011. Detection and quantification of rare mutations with massively parallel sequencing. *Proc Natl Acad Sci* **108:** 9530–9535. doi:10.1073/pnas.1105422108

Kohler S, Vasilevsky NA, Engelstad M, Foster E, McMurry J, Ayme S, Baynam G, Bello SM, Boerkoel CF, Boycott KM, et al. 2017. The Human Phenotype Ontology in 2017. *Nucleic Acids Res* **45:** D865–D876. doi:10.1093/nar/gkw1039

Kothur K, Holman K, Farnsworth E, Ho G, Lorentzos M, Troedson C, Gupta S, Webster R, Procopis PG, Menezes MP, et al. 2018. Diagnostic yield of targeted massively parallel sequencing in children with epileptic encephalopathy. *Seizure* **59:** 132–140. doi:10.1016/j.seizure.2018.05.005

Krupp DR, Barnard RA, Duffourd Y, Evans SA, Mulqueen RM, Bernier R, Riviere JB, Fombonne E, O'Roak BJ. 2017. Exonic mosaic mutations contribute risk for autism spectrum disorder. *Am J Hum Genet* **101:** 369–390. doi:10.1016/j.ajhg.2017.07.016

Lee H, Deignan JL, Dorrani N, Strom SP, Kantarci S, Quintero-Rivera F, Das K, Toy T, Harry B, Yourshaw M, et al. 2014. Clinical exome sequencing for genetic identification of rare Mendelian disorders. *J Am Med Assoc* **312:** 1880–1887. doi:10.1001/jama.2014.14604

Lim ET, Uddin M, De Rubeis S, Chan Y, Kamumbu AS, Zhang X, D'Gama AM, Kim SN, Hill RS, Goldberg AP, et al. 2017. Rates, distribution and implications of postzygotic mosaic mutations in autism spectrum disorder. *Nat Neurosci* **20:** 1217–1224. doi:10.1038/nn.4598

Lindhurst MJ, Sapp JC, Teer JK, Johnston JJ, Finn EM, Peters K, Turner J, Cannons JL, Bick D, Blakemore L, et al. 2011. A mosaic activating mutation in *AKT1* associated with the Proteus syndrome. *N Engl J Med* **365:** 611–619. doi:10.1056/NEJMoa1104017

Louie RJ, Friez MJ, Skinner C, Baraitser M, Clark RD, Schwartz CE, Stevenson RE. 2020. Clark–Baraitser syndrome is associated with a nonsense alteration in the autosomal gene *TRIP12*. *Am J Med Genet* **182:** 595–596. doi:10.1002/ajmg.a.61443

Madsen RR, Vanhaesebroeck B, Semple RK. 2018. Cancer-associated *PIK3CA* mutations in overgrowth disorders. *Trends Mol Med* **24:** 856–870. doi:10.1016/j.molmed.2018.08.003

Mandelker D, Schmidt RJ, Ankala A, McDonald Gibson K, Bowser M, Sharma H, Duffy E, Hegde M, Santani A, Lebo M, et al. 2016. Navigating highly homologous genes in a molecular diagnostic setting: a resource for clinical next-generation sequencing. *Genet Med* **18:** 1282–1289. doi:10.1038/gim.2016.58

Masliah-Plachon J, Auvin S, Nectoux J, Fichou Y, Chelly J, Bienvenu T. 2010. Somatic mosaicism for a *CDKL5* mutation as an epileptic encephalopathy in males. *Am J Med Genet A* **152A:** 2110–2111. doi:10.1002/ajmg.a.33037

Mei D, Darra F, Barba C, Marini C, Fontana E, Chiti L, Parrini E, Dalla Bernardina B, Guerrini R. 2014. Optimizing the molecular diagnosis of *CDKL5* gene–related epileptic encephalopathy in boys. *Epilepsia* **55:** 1748–1753. doi:10.1111/epi.12803

Meng L, Pammi M, Saronwala A, Magoulas P, Ghazi AR, Vetrini F, Zhang J, He W, Dharmadhikari AV, Qu C, et al. 2017. Use of exome sequencing for infants in intensive care units: ascertainment of severe single-gene disorders and effect on medical management. *JAMA Pediatr* **171:** e173438. doi:10.1001/jamapediatrics.2017.3438

Mignot C, McMahon AC, Bar C, Campeau PM, Davidson C, Buratti J, Nava C, Jacquemont ML, Tallot M, Milh M, et al. 2019. *IQSEC2*-related encephalopathy in males and females: a comparative study including 37 novel patients. *Genet Med* **21:** 837–849. doi:10.1038/s41436-018-0268-1

Mirzaa GM, Conti V, Timms AE, Smyser CD, Ahmed S, Carter M, Barnett S, Hufnagel RB, Goldstein A, Narumi-Kishimoto Y, et al. 2015. Characterisation of mutations of the phosphoinositide-3-kinase regulatory subunit, *PIK3R2*, in perisylvian polymicrogyria: a next-generation sequencing study. *Lancet Neurol* **14:** 1182–1195. doi:10.1016/S1474-4422(15)00278-1

Nambot S, Thevenon J, Kuentz P, Duffourd Y, Tisserant E, Bruel AL, Mosca-Boidron AL, Masurel-Paulet A, Lehalle D, Jean-Marcais N, et al. 2018. Clinical whole-exome sequencing for the diagnosis of rare disorders with congenital anomalies and/or intellectual disability: substantial interest of prospective annual reanalysis. *Genet Med* **20:** 645–654. doi:10.1038/gim.2017.162

Olson HE, Demarest ST, Pestana-Knight EM, Swanson LC, Iqbal S, Lal D, Leonard H, Cross JH, Devinsky O, Benke TA. 2019. Cyclin-dependent kinase-like 5 deficiency disorder: clinical review. *Pediatr Neurol* **97:** 18–25. doi:10.1016/j.pediatrneurol.2019.02.015

Poirier K, Abriol J, Souville I, Laroche-Raynaud C, Beldjord C, Gilbert B, Chelly J, Bienvenu T. 2005. Maternal mosaicism for mutations in the *ARX* gene in a family with X linked mental retardation. *Hum Genet* **118:** 45–48. doi:10.1007/s00439-005-0011-2

Radley JA, O'Sullivan RBG, Turton SE, Cox H, Vogt J, Morton J, Jones E, Smithson S, Lachlan K, Rankin J, et al. 2019. Deep phenotyping of 14 new patients with *IQSEC2* variants, including monozygotic twins of discordant phenotype. *Clin Genet* **95:** 496–506. doi:10.1111/cge.13507

Retterer K, Juusola J, Cho MT, Vitazka P, Millan F, Gibellini F, Vertino-Bell A, Smaoui N, Neidich J, Monaghan KG, et al. 2016. Clinical application of whole-exome sequencing across clinical indications. *Genet Med* **18:** 696–704. doi:10.1038/gim.2015.148

Richards S, Aziz N, Bale S, Bick D, Das S, Gastier-Foster J, Grody WW, Hegde M, Lyon E, Spector E, et al. 2015. Standards and guidelines for the interpretation of sequence variants: a joint consensus recommendation of the American College of Medical Genetics and Genomics and the Association for Molecular Pathology. *Genet Med* **17:** 405–424. doi:10.1038/gim.2015.30

Riviere JB, Mirzaa GM, O'Roak BJ, Beddaoui M, Alcantara D, Conway RL, St-Onge J, Schwartzentruber JA, Gripp KW, Nikkel SM, et al. 2012. De novo germline and postzygotic mutations in *AKT3*, *PIK3R2* and *PIK3CA* cause a spectrum of related megalencephaly syndromes. *Nat Genet* **44:** 934–940. doi:10.1038/ng.2331

Robinson JT, Thorvaldsdottir H, Winckler W, Guttman M, Lander ES, Getz G, Mesirov JP. 2011. Integrative genomics viewer. *Nat Biotechnol* **29:** 24–26. doi:10.1038/nbt.1754

Santen GW, Aten E, Vulto-van Silfhout AT, Pottinger C, van Bon BW, van Minderhout IJ, Snowdowne R, van der Lans CA, Boogaard M, Linssen MM, et al. 2013. Coffin–Siris syndrome and the BAF complex: genotype–phenotype study in 63 patients. *Hum Mutat* **34:** 1519–1528. doi:10.1002/humu.22394

Schmitt MW, Kennedy SR, Salk JJ, Fox EJ, Hiatt JB, Loeb LA. 2012. Detection of ultra-rare mutations by next-generation sequencing. *Proc Natl Acad Sci* **109:** 14508–14513. doi:10.1073/pnas.1208715109

Shirley MD, Tang H, Gallione CJ, Baugher JD, Frelin LP, Cohen B, North PE, Marchuk DA, Comi AM, Pevsner J. 2013. Sturge–Weber syndrome and port-wine stains caused by somatic mutation in *GNAQ*. *N Engl J Med* **368:** 1971–1979. doi:10.1056/NEJMoa1213507

Shoubridge C, Fullston T, Gecz J. 2010. *ARX* spectrum disorders: making inroads into the molecular pathology. *Hum Mutat* **31:** 889–900. doi:10.1002/humu.21288

Shoubridge C, Tan MH, Seiboth G, Gecz J. 2012. ARX homeodomain mutations abolish DNA binding and lead to a loss of transcriptional repression. *Hum Mol Genet* **21:** 1639–1647. doi:10.1093/hmg/ddr601

Stark Z, Tan TY, Chong B, Brett GR, Yap P, Walsh M, Yeung A, Peters H, Mordaunt D, Cowie S, et al. 2016. A prospective evaluation of whole-exome sequencing as a first-tier molecular test in infants with suspected monogenic disorders. *Genet Med* **18:** 1090–1096. doi:10.1038/gim.2016.1

Stosser MB, Lindy AS, Butler E, Retterer K, Piccirillo-Stosser CM, Richard G, McKnight DA. 2018. High frequency of mosaic pathogenic variants in genes causing epilepsy-related neurodevelopmental disorders. *Genet Med* **20:** 403–410. doi:10.1038/gim.2017.114

Tsurusaki Y, Okamoto N, Ohashi H, Kosho T, Imai Y, Hibi-Ko Y, Kaname T, Naritomi K, Kawame H, Wakui K, et al. 2012. Mutations affecting components of the SWI/SNF complex cause Coffin–Siris syndrome. *Nat Genet* **44:** 376–378. doi:10.1038/ng.2219

Wieczorek D, Bogershausen N, Beleggia F, Steiner-Haldenstatt S, Pohl E, Li Y, Milz E, Martin M, Thiele H, Altmuller J, et al. 2013. A comprehensive molecular study on Coffin–Siris and Nicolaides–Baraitser syndromes identifies a broad molecular and clinical spectrum converging on altered chromatin remodeling. *Hum Mol Genet* **22:** 5121–5135. doi:10.1093/hmg/ddt366

Yang Y, Muzny DM, Reid JG, Bainbridge MN, Willis A, Ward PA, Braxton A, Beuten J, Xia F, Niu Z, et al. 2013. Clinical whole-exome sequencing for the diagnosis of mendelian disorders. *N Engl J Med* **369:** 1502–1511. doi:10.1056/NEJMoa1306555

Yang Y, Muzny DM, Xia F, Niu Z, Person R, Ding Y, Ward P, Braxton A, Wang M, Buhay C, et al. 2014. Molecular findings among patients referred for clinical whole-exome sequencing. *J Am Med Assoc* **312:** 1870–1879. doi:10.1001/jama.2014.14601

Zhang J, Gambin T, Yuan B, Szafranski P, Rosenfeld JA, Balwi MA, Alswaid A, Al-Gazali L, Shamsi AMA, Komara M, et al. 2017. Haploinsufficiency of the E3 ubiquitin-protein ligase gene *TRIP12* causes intellectual disability with or without autism spectrum disorders, speech delay, and dysmorphic features. *Hum Genet* **136:** 377–386. doi:10.1007/s00439-017-1763-1